

**MULTISPECTRAL STUDY OF MAJOR SOLAR  
FLARES TOWARD FLARES PREDICTIONS**

**MUHAMAD AKRAM ZAKI BIN ROSLAN**

**UNIVERSITI SAINS MALAYSIA**

**2018**

**MULTISPECTRAL STUDY OF MAJOR SOLAR  
FLARES TOWARD FLARES PREDICTIONS**

by

**MUHAMAD AKRAM ZAKI BIN ROSLAN**

**Thesis submitted in fulfillment of the requirements  
for the degree of  
Master of Science**

**SEPTEMBER 2018**

## ACKNOWLEDGEMENT

Indeed, in the creation of the heavens and the Earth and the alternation of the night and the day are signs for those of understanding (190). Who remember Allah while standing or sitting or (lying) on their sides and give thought to the creation of the heavens and the earth, (saying), "Our Lord, You did not create this aimlessly; exalted are You (above such a thing), then protect us from the punishment of the Fire (191). [Al-Quran 3:190-191].

In the name of Allah, Most Gracious, Most Merciful. First, I am grateful and thankful to Allah S.W.T and Prophet Muhammad S.A.W forgiveness of mercy and guidance to complete this research in the glorious month of Ramadhan.

I would also like to thank my parents and family for praying for my success. Not forgetting my respected supervisor, Professor Madya Dr Abdul Halim Bin Abdul Aziz for the guidance, encouragement, enthusiasm and patient was given during this research. I would like to acknowledge National Geophysical Data Center (NGDC) and Solar and Heliospheric Observatory (SOHO) agency for providing public archive data.

I would like to thank my colleagues (Aummmm members, Jade View members, and Seniors) especially Dr Suhana Arshad for giving me the guidance and motivation of my life in USM. I also would like to acknowledge Universiti Sains Malaysia (USM) especially School of Physics for providing a platform to conduct this study.

## TABLE OF CONTENTS

<b>ACKNOWLEDGEMENT</b>	<b>ii</b>
<b>TABLE OF CONTENTS</b>	<b>iii</b>
<b>LIST OF TABLES</b>	<b>ix</b>
<b>LIST OF FIGURES</b>	<b>xi</b>
<b>LIST OF ABBREVIATIONS</b>	<b>xx</b>
<b>ABSTRAK</b>	<b>xxii</b>
<b>ABSTRACT</b>	<b>xxiv</b>
<b>CHAPTER 1 – INTRODUCTION</b>	<b>1</b>
1.1 Introduction of the Sun	1
1.1.2 Structure of the Sun	1
1.2 Space weather	4
1.3 Problems statement	5
1.4 Research objectives	6
1.5 Research scope	6
1.6 Thesis layout	7
<b>CHAPTER 2 – LITERATURE REVIEW</b>	<b>9</b>
2.1 Solar activities	9
2.1.1 Active Region (AR) and Sunspots	12
2.1.1(a) Zurich Classifications Systems	12
2.1.1(b) McIntosh Classifications Systems	12
2.1.1(b)(i) Modified Zurich Class – Z	14

2.1.1(b)(ii)	Penumbra Class – P	15
2.1.1(c)(iii)	Compactness Class – C	16
2.1.1(c)	Mount Wilson Classifications	19
2.1.2	Relationship between McIntosh and Mt Wilson Class towards major flares	21
2.2	Solar flares	23
2.2.1	The theories of Solar eruptions	25
2.1.2	The theories of Solar flares	26
2.1.3	The magnetic flux rope (MFRs)	35
2.1.4	The sigmoidal shapes	41
2.3	The relationship between solar flares and CMEs	45
2.4	Monitoring and prediction of Solar activities	48
<b>CHAPTER 3 - DATA COLLECTION AND METHODOLOGY</b>		<b>51</b>
3.1	Introduction	51
3.2	National Geophysical Data Centre (NGDC)	54
3.2.1	Sunspot regions Catalogue	55
3.2.2	X-ray Catalogue	55
3.2.3	Data Processing	55
3.3	Solar and Heliospheric Observatory (SOHO)	60
3.3.1	Continuum Images	62
3.3.1	Magnetogram Images	64
3.3.1	Extreme Ultraviolet Images Telescopes (EIT 195Å)	65
3.4	Images Analysis	66
3.4.1	Continuum Images	68

3.4.2	Magnetogram Images	69
3.4.3	Extreme Ultraviolet Images Telescopes (EIT 195Å)	70
3.5	Prediction Method	72
3.6	Chapter summary	72
<b>CHAPTER 4 – RESULTS AND DISCUSSIONS</b>		<b>74</b>
4.1	Introduction	74
4.2	The X-ray intensity of Active Regions (AR)	75
4.2.1	X-ray Intensity of AR 9077	75
4.2.2	X-ray Intensity of AR 9393	76
4.2.3	X-ray Intensity of AR 9415	77
4.2.4	X-ray Intensity of AR 10486	78
4.2.5	X-ray Intensity of AR 10720	80
4.2.6	The Relationship X-ray intensity and major solar flares	81
4.3	The area evolution of Active Regions	82
4.3.1	The area evolution of active regions AR 9077	82
4.3.2	The area evolution of active regions AR 9393	83
4.3.3	The area evolution of active regions AR 9415	85
4.3.4	The area evolution of active regions AR 10486	87
4.3.5	The area evolution of active regions AR 10720	88
4.3.6	The relationship of active regions and major Solar flares	90
4.4	The evolution of Zurich Class in active regions	90
4.4.1	The evolution of Zurich Class in AR 9077	90
4.4.2	The evolution of Zurich Class in AR 9393	91
4.4.3	The evolution of Zurich Class in AR 9415	92

4.4.4	The evolution of Zurich Class in AR 10486	93
4.4.5	The evolution of Zurich Class in AR 10720	95
4.4.6	The relationships of Zurich Class and major Solar flares	96
4.5	The evolution of Penumbra Class in active regions	98
4.5.1	The evolution of Penumbra Class in AR 9077	98
4.5.2	The evolution of Penumbra Class in AR 9393	99
4.5.3	The evolution of Penumbra Class in AR 9415	100
4.5.4	The evolution of Penumbra Class in AR 10486	100
4.5.5	The evolution of Penumbra Class in AR 10720	101
4.5.6	The relationship of Penumbra Class and major Solar flares	102
4.6	The evolution of Compactness Class in active regions	103
4.6.1	The evolution of Compactness Class in AR 9077	103
4.6.2	The evolution of Compactness Class in AR 9393	104
4.6.3	The evolution of Compactness Class in AR 9415	105
4.6.4	The evolution of Compactness Class in AR 10486	106
4.6.5	The evolution of Compactness Class in AR 10720	107
4.6.6	The relationship of Compactness Class and major Solar flares	108
4.7	The evolution of Mt Wilson Class in Active Regions	109
4.7.1	The evolution of Mt Wilson Class in AR 9077	109
4.7.2	The evolution of Mt Wilson Class in AR 9393	110
4.7.3	The evolution of Mt Wilson Class in AR 9415	111
4.7.4	The evolution of Mt Wilson Class in AR 10486	112
4.7.5	The evolution of Mt Wilson Class in AR 10720	114
4.7.6	The relationship of Mt Wilson Class Major Solar flares	115

4.8	The Multispectral Images of Major Solar Flares in AR 9077	117
4.8.1	Solar Flares X1.9	117
4.8.2	Solar Flares X5.7	118
4.9	The Multispectral Images of Major Solar Flares in AR 9393	120
4.9.1	Solar Flares X1.7	120
4.9.2	Solar Flares X1.4	122
4.9.3	Solar Flares X20.0	124
4.10	The Multispectral Images of Major Solar Flares in AR 9415	126
4.10.1	Solar Flares X1.2	128
4.10.2	Solar Flares X5.6	131
4.10.3	Solar Flares X2.3	130
4.10.4	Solar Flares X2.0	131
4.10.5	Solar Flares X14.4	133
4.11	The Multispectral Images of Major Solar Flares in AR 10486	135
4.11.1	Solar Flares X5.4	135
4.11.2	Solar Flares X1.1	137
4.11.3	Solar Flares X17.2	139
4.11.4	Solar Flares X10.0	141
4.11.5	Solar Flares X8.3	143
4.11.6	Solar Flares X28.0	145
4.12	The Multispectral Images of Major Solar Flares in AR 10720	147
4.12.1	Solar Flares X1.2	147
4.12.2	Solar Flares X2.6	149
4.12.3	Solar Flares X3.8	151
4.12.4	Solar Flares X1.3	153



4.12.5	Solar Flare X7.1	155
4.13	The Relationship of Multispectral Images and Major Solar Flares	157
4.14	The Prediction Method of Major Solar Flares	160
4.14.1	The Model Testing and Results	161
4.14.2	The Images of Major Solar Flares	164
<b>CHAPTER 5 – CONCLUSION AND RECOMENDATION</b>		166
5.1	Conclusions	166
5.1	Recommendation	167
<b>REFERENCES</b>		169
<b>APPENDIX A</b>		

## LIST OF TABLES

		<b>Page</b>
Table 2.1	The definition of modified Zurich class (AFWAMAN, 2003).	14
Table 2.2	The definition of Penumbra class (AFWAMAN, 2003).	16
Table 2.3	The definition of Compactness class (AFWAMAN, 2003).	17
Table 2.4	Allowed types group in McIntosh classification system (AFWAMAN, 2003)	17
Table 2.5	The definition of Mt Wilson class (AFWAMAN, 2003)	19
Table 2.6	The solar flares class and its effects toward Earth	24
Table 3.1	List of the active region and major solar flares.	52
Table 3.2	Data processing level on MDI images (Bogart, 2014) (SOHO, 2014).	63
Table 4.1	Solar flares class in AR 10486 and it counts.	76
Table 4.2	Solar flares class in AR 9393 and it counts.	77
Table 4.3	Solar flares class in AR 9415 and it counts.	78
Table 4.4	Solar flares class in AR 10720 and it counts.	79
Table 4.5	Solar flares class in AR 9077 and it counts.	80
Table 4.6	Solar flares count in five active regions.	81
Table 4.7	Major solar flares intensity and its area in AR 10486.	84
Table 4.8	Major solar flares and its area in AR 9393.	84
Table 4.9	Major solar flares and its area in AR 9415.	86
Table 4.10	Major solar flares and its area in AR 10720.	88
Table 4.11	Major solar flare intensity and Zurich class AR 10486.	93
Table 4.12	Major solar flares Intensity and Zurich class AR 9415.	94

Table 4.13	Major solar flares intensity and Zurich class AR 10720.	96
Table 4.14	Major solar flares count on Zurich class.	97
Table 4.15	Major solar flares count on Compactness class.	109
Table 4.16	Major solar flares intensity and Mt Wilson class AR 9415.	112
Table 4.17	Major solar flares intensity and Mt Wilson class AR 10720.	115
Table 4.18	Major solar flares count on Mt Wilson Class.	116
Table 4.19	The measurement of magnetic flux rope, sigmoidal shape, arcade formation and Magnetic loop.	159
Table 4.20	The selected criteria for major solar flares.	161
Table 4.21	The definition of conditions.	162
Table 4.22	Conditions and values of the samples classifications.	164
Table 4.23	Model classification, definition, formula and results.	164
Table 4.24	The images spectrum and features of solar flares.	165

## LIST OF FIGURES

		<b>Page</b>
Figure 1.1	Structure of the Sun (Nasa 2017).	3
Figure 2.1	The central dark part of the sunspots is the umbra. The radially striated part is the penumbra. The surrounding bright cells are granular convection cells (Solanki, 2003).	11
Figure 2.2	The 3 component McIntosh classification with examples of each category. The first column is Zurich class, the second column is Penumbra class and the third column is Compactness class (Nguyen et al. 2006).	13
Figure 2.3	Sunspots group length measurement and penumbra diameter (AFWAMAN, 2003).	15
Figure 2.4	Example Mt Magnetic classification system.	20
Figure 2.5	The example of solar flares event on (i) schematic picture of CSHKP model (H. S. Hudson 2011) and (ii) the large cusp structure of solar flares (M3.3) observed several hours after the impulsive peak capture by Yohkoh/SXT and reported by Yokoyama et al. (2001).	27
Figure 2.6	The example of solar flares event on (i) Soft X-ray image of a long decay event (LDE) flare observed by Yohkoh on February 21, 1992 (Magara and Shibata 2008) and (ii) schematic picture of a large-scale eruption such as an LDE flare and CME (K. Shibata et al. 1995; Kazunari Shibata 1998). This schematic diagram is similar to CSHKP model.	28
Figure 2.7	Schematic picture of the plasmoid-induced reconnection for Large-scale eruption proposed by Shibata (1998) (Magara and Shibata, 2008).	29
Figure 2.8	Plasmoid reconnection process proposed by Shibata (1998). (a) and (b) is the large-scale eruption. (a) pre-	30

eruptive state and (b) post-eruptive state. While (c) and (d) Small-scale eruption (c) pre-eruptive state; (d) post-eruptive state. (Magara and Shibata, 2008)

Figure 2.9	The basics of magnetic field configuration before on set (a), during onset (b), ejective eruption (c) and after of set and confined structure of solar flares (d). The dashed curve is the photospheric polarity inversion line, PIL (the line dividing between the two opposite-polarity). It appears like sigmoidal S shape. The diagonally lined features above the PIL in the (a) is the filament that is often present in sheared core fields. The grey areas in (c) and (d) are ribbons of flare emission in the lower atmosphere. It is the feet of magnetic field line origin (Moore et al., 2001).	32
Figure 2.10	The magnetic field line at feet points is anchored in the photosphere. “Bc” refers to magnetic loop in the corona (Moore et al., 2001). A simple “shearing” motion of the feet points (v) lead to produce eruptions (Moore et al., 2001).	33
Figure 2.11	The formation of MFR by using MHD simulations. Time is the unit of Alfven time (Amari et al., 2000).	37
Figure 2.12	Top view of MFR during (a) $t = 400$ and (b) $t = 430$ . At $t = 400$ , the MFR shows inverse J structures while at $t = 430$ the MFR shows single S structures. (Amari et al., 2000)	38
Figure 2.13	The example of sigmoidal shape (as black) in Yohkoh SXT image shows during the pre-flare (Hudson and Fletcher, 2004).	42
Figure 2.14	Pre-flares of solar flares C4.7 on 9/3/2012 as observed by AIA304Å (left column), AIA171Å (middle) and AIA131 Å (right) (Polito, V. et al., 2017).	43
Figure 2.15	Solar flares phases in EIT 195Å (EUV) images during solar flare X17 on AR 10720 on 28/10/2003 (Krall et al., 2006).	43

Figure 2.16	A arcade formation after solar flares X2.3 (left, 171Å) (Fletcher et al., 2011) and X5.4 (right, 195Å) (Hudson and Fletcher, 2004).	44
Figure 2.17	Solar flares-CMEs associations rate (%) of 778 events (Youssef, 2012).	46
Figure 2.18	Solar flares observe by EIT 195Å (left) and LASCO (right) (Gopalswamy, 2010).	47
Figure 2.19	Example similarity location between solar flares and CMES in EIT 195Å (left) and LASCO (right) (Gopalswamy, 2010).	47
Figure 3.1	Research flowchart.	53
Figure 3.2	The of an example of the complexity of the dataset and (ii) arrangement of data by using Microsoft Excel 2016.	56
Figure 3.3	The example of X-ray intensity of all solar flares in AR 10486. The blue “dot” refers to major solar flares. The intensity axis was plotted in the log scale.	57
Figure 3.4	The example of active regions area AR 10486. The blue “dot” refers to major solar flares.	58
Figure 3.5	The example of evolution Zurich class in AR 10486. The blue “dot” is referring to major solar flares.	58
Figure 3.6	The example of evolution Penumbra class in AR 10486. The blue “dot” is referring to major solar flares.	59
Figure 3.7	The example of evolution Compactness class in AR 10486. The blue “dot” is referring to major solar flares.	59
Figure 3.8	The example of evolution Mt Wilson class in AR 10486. The blue “dot” is referring to major solar flares.	60

Figure 3.9	The example interfaces for SOHO website for (i) data request and (ii) data product.	62
Figure 3.10	The continuum images on (i) 28/10/2003 and (ii) 14/07/2000.	64
Figure 3.11	The continuum images on 28/10/2003 (left) and 14/07/2000 (right).	65
Figure 3.12	The EIT 195Å images on (i) 28/10/2003 and (ii) 14/07/2000.	66
Figure 3.13	The example of image opened by ImageJ. The adjustment of brightness and contrast at the right panel.	67
Figure 3.14	The example of the images opened by Helio Images Viewer. The left panel is the coordinates detail.	68
Figure 3.15	Zoom-in example image of an active region.	69
Figure 3.16	Zoom in examples of MFR images in 3 different AR. The blue line indicate the length measurement.	70
Figure 3.17	The example of solar flares phases for solar flare X5.7 in AR 9077. The blue line indicate length measurement. During the impulsive phase, CCD become saturated and bleeding to another pixel.	71
Figure 4.1	X-ray intensity of all solar flares in AR 9077. The blue “dot” refers to major solar flares. The black line on 12/7/2000 is to differentiate between the growth and decay phase of AR (left is growth while the right is decay).	75
Figure 4.2	X-ray intensity of all solar flares in AR 9393. The blue “dot” refers to major solar flares. The black line on 31/03/2001 is to differentiate between the growth and decay phase of active regions.	76
Figure 4.3	X-ray intensity of all solar flares in AR 9415. The blue “dot” refers to major solar flares. The black line on 8/04/2001 is to differentiate between the growth and decay phase of AR.	77

Figure 4.4	X-ray intensity of all solar flares in AR 10486. The blue “dot” refers to major solar flares. The black line on 30/10/2003 is to differentiate between the growth and decay phase of AR .	79
Figure 4.5	X-ray intensity of all solar flares in AR 10720. The blue “dot” refers to major solar flares. The black line on 16/01/2005 is to differentiate between the growth and decay phase of AR.	80
Figure 4.6	The evolution area of AR 9077. The blue “dot” is referring to major flares.	82
Figure 4.7	The evolution area of AR 9393. The blue “dot” is referring to major flares.	83
Figure 4.8	The evolution area of AR 9415. The blue “dot” is referring to major flares.	85
Figure 4.9	The evolution area of AR 10486. The blue “dot” referring to major flares.	86
Figure 4.10	The evolution area of AR 10720. The blue “dot” is referring to major flares.	87
Figure 4.11	The relationship of total major solar flares and AR area.	89
Figure 4.12	Figure 4.1: The evolution of Zurich Class of AR 9077. The blue “dot” is referring to major solar flares.	90
Figure 4. 13	The evolution of Zurich class in AR 9393. The blue “dot” is referring to major solar flares.	91
Figure 4.14	The evolution of Zurich class in AR 9415. The blue “dot” is referring to major solar flares.	92
Figure 4.15	The evolution of Zurich class in AR 10486. The blue “dot” is referring to major solar flares.	94



Figure 4.16	The evolution of Zurich class in AR 10720. The blue “dot” is referring to major solar flares	95
Figure 4.17	The relationship between Zurich class and total major solar flares.	97
Figure 4.18	The evolution of Penumbra class in AR 9077. The blue “dot” is referring to major solar flares.	98
Figure 4.19	The evolution of penumbra class in AR 9393. The blue “dot” is referring to major solar flares.	99
Figure 4.20	The evolution of the Penumbra class in AR 9415. The blue “dot” is referring to major solar flares.	100
Figure 4.21	The evolution of Penumbra class in AR 10486. The blue “dot” is referring to major solar flares.	101
Figure 4.22	The evolution of Penumbra Class in AR 10720. The blue “dot” is referring to major solar flares.	102
Figure 4.23	The relationship of Penumbra class and total major solar flares.	103
Figure 4.24	The evolution of Compactness class in AR 9077. The blue “dot” is referring to major solar flares.	104
Figure 4.25	The evolution of Compactness class in AR 9393. The blue “dot” is referring to major solar flares.	105
Figure 4.26	The evolution of Compactness class in AR 9415. The blue “dot” is referring to major solar flares.	106
Figure 4.27	The evolution of Compactness class in AR 10486. The blue “dot” is referring to major solar flares.	107
Figure 4.28	The evolution of Compactness class in AR 10720. The blue “dot” is referring to major solar flares.	108
Figure 4.29	The relationship Compactness class and total major solar flare.	109

Figure 4.30	The evolution of Mt Wilson class in AR 9077. The blue “dot” is referring to major solar flares.	111
Figure 4.31	The evolution of Mt Wilson class in AR 9393. The blue “dot” is referring to major solar flares.	112
Figure 4.32	The evolution of Mt Wilson class in AR 9415. The blue “dot” is referring to major solar flares	113
Figure 4.33	The evolution of Mt Wilson class in AR 10486. The blue “dot” is referring to major solar flares.	114
Figure 4.34	The evolution of Mt Wilson class in AR 9077. The blue “dot” is referring to major solar flares. 116	115
Figure 4.35	The relationship between Mt Wilson magnetic class and total major solar flares.	117
Figure 4.36	Images of AR 9077 and solar flare X1.9 in (i) continuum and (ii) magnetogram spectrum. The solar flare occurs at 10:37 UT on 12/07/2000. The EIT 195 Å for this image is not available.	118
Figure 4.37	Images of AR 9077 and solar flare X5.7 in (i) continuum, (ii) magnetogram (iii) and EIT 195Å spectrum. The solar flare occurs at 10:24 UT on 12/07/2000.	120
Figure 4.38	Images of AR 9393 and solar flares X1.7 in (i) continuum, (ii) magnetogram and (iii) EIT 195Å spectrum. The solar flare occurs at 10:14 UT on 29/3/2001.	122
Figure 4.39	Images of AR 9393 and solar flares X1.4 in (i) continuum, (ii) magnetogram and (iii) EIT 195Å spectrum. The solar flare occurs at 10:14 UT on 2/4/2001.	124
Figure 4.40	Images of AR 9393 and solar flares X20.0 in continuum (i), magnetogram (ii) and EIT 195Å (iii) spectrum. The solar flare occurs at 21:48 UT on 2/4/2001.	126

Figure 4.41	Images of AR 9415 and solar flares X1.2 in (i) continuum, (ii) magnetogram and (iii) EIT 195Å spectrum. The solar flare occurs at 04:00UT on 3/4/2001.	128
Figure 4.42	Images of AR 9415 and solar flares X5.6 in (i) continuum, (ii) magnetogram and (iii) EIT 195Å spectrum. The solar flare occurs at 19:24 UT on 6/4/2001.	130
Figure 4.43	Images of AR 9415 and solar flares X2.3 in continuum (i) and magnetogram (ii). The solar flares occur at 5:26 on 10/4/2001. EIT 195Å is not available.	131
Figure 4.44	Images of AR 9415 and solar flare X2.0 in continuum (i), magnetogram (ii) and EIT 195Å (iii) spectrum. The solar flares occur at 10:25 UT on 12/4/2001.	133
Figure 4.45	Images of AR 9415 and solar flare X14.4 in continuum (i), magnetogram (ii) and EIT 195Å (iii) spectrum. The solar flares occur at 13:48 UT on 15/4/2001.	135
Figure 4.46	Images of AR 10486 and solar flare X5.4 in (i) continuum, (ii) magnetogram and (iii) EIT 195Å spectrum. The solar flare occurs at 8:36 UT on 23/10/2003.	137
Figure 4.47	Images of AR 10486 and solar flare X1.1 in (i) continuum, (ii) magnetogram and (iii) EIT 195Å spectrum. The solar flare occurs at 20:12UT on 23/10/2003.	149
Figure 4.48	Images of AR 10486 and solar flare X17.2 in (i) continuum, (ii) magnetogram and (iii) EIT 195Å spectrum. The solar flare occurs at 11:12 UT on 28/10/2003.	141
Figure 4.49	Images of AR 10486 and solar flares X10.0 in (i) continuum, (ii) magnetogram and (iii) EIT 195Å	143

	spectrum. The solar flare occurs at 20:48 UT on 29/10/2003.	
Figure 4.50	Images of AR 10486 and solar flare X8.3 in (i) continuum, (ii) magnetogram and (iii) EIT 195Å spectrum. The solar flare occurs at 17:12 UT on 2/11/2003	145
Figure 4.51	Images of AR 10486 and solar flare X28.0 in (i) continuum, (ii) magnetogram and (iii) EIT 195Å spectrum. The solar flare occurs at 19:48 UT on 4/11/2003.	147
Figure 4.52	Images of AR 10720 and solar flares X1.2 in (i) continuum, (ii) magnetogram and (iii) EIT 195Å spectrum. The solar flare occurs at 00:48 UT on 15/01/2001.	149
Figure 4.53	Images of AR 10720 and solar flare X2.6 in (i) continuum, (ii) magnetogram and (iii) EIT 195Å spectrum. The solar flare occurs at 23:12 UT on 15/01/2001.	151
Figure 4.54	Images of AR 10720 and solar flares X3.8 in (i) continuum, (ii) magnetogram and (iii) EIT 195Å spectrum. The solar flare occurs at 10:00 UT on 17/01/2005.	153
Figure 4.55	Images of AR 10720 and solar flare X1.3 in (i) continuum, (ii) magnetogram and (iii) EIT 195Å spectrum. The solar flare occurs at 8:23 UT on 19/01/2001.	155
Figure 4.56	Images of AR 10720 and solar flare X7.1 in (i) continuum, (ii) magnetogram and (iii) EIT 195Å spectrum. The solar flare occurs at 6:48 UT on 20/01/2005.	157
Figure 4.57	Schematic map for sample classification.	163

## LIST OF ABBREVIATIONS

ASAP	Automated Solar Activity Prediction
AI	Artificial Intelligent
AR	Active Region
CME	Coronal Mass Ejection
EIT	Extreme Ultraviolet Imaging Telescopes
EM	Electromagnetic
EUV	Extreme Ultraviolet
FITS	Flexible Image Transport System
LEO	Low Earth Orbiting
LASCO	Large Angle and Spectrometric Coronagraph
GOES	Geostationary Operational Environmental Satellite
MFR	Magnetic Flux Rope
SEP	Solar Energetic Particles
PIL	Polarity Inversion Lines
Xrs	X-ray sensor
SXR	Soft X-ray
HXR	Hard X-ray
ESA	Europe Space Agency
NASA	National Aeronautics and Space Administration
SOHO	Solar and Heliospheric Observatory
NGDC	National Geophysical Data Center
NOAA	National Oceanic and Atmospheric Administration
NLFFF	Non-linear force-free field

GPS	Global Positioning System
USAF/MWL	United States Air Force/Mount Wilson
SWPC	Space Weather Prediction System
Zpc	Zurich, Penumbra, Compactness
TP	True Positive
TN	True Negative
FP	False Positive
FN	False Negative

# **KAJIAN BERBILANG SPEKTRUM SUAR SURIA UTAMA UNTUK RAMALAN SUAR UTAMA**

## **ABSTRAK**

Suar suria utama (X-Class) adalah aktiviti suria yang paling berbahaya kepada Bumi dari segi cuaca angkasa. Ia disebabkan oleh letusan magnetik dan pelepasan tenaga magnetik matahari secara mendadak di kawasan aktif. Objektif utama penyelidikan ini adalah untuk mengenal pasti ciri-ciri kawasan aktif (kelas McIntosh dan kelas Mt Wilson) yang berkaitan dengan suar utama dari NGDC data dan untuk merangka kriteria bagi ramalan awal. Kriteria ini dipertingkatkan oleh imej berbilang spektrum kualitatif. Imej berbilang spektrum seperti keselenjaraan, magnetogram, dan imej EIT 195Å dari SOHO digunakan dalam kajian ini. Kajian ini mengambil kira evolusi AR, sifat AR (Zurich, Penumbra, Compactness dan kelas Mt Wilson), morfologi tali fluks magnetik (MFR), dan pembentukan bentuk sigmoid magnetik. Mengambil kira kesediaan dan konsistensi data, lima AR iaitu AR 10486, AR 9393, AR 9415, AR 10720 dan AR 9077 telah dipilih. Setiap AR menghasilkan beberapa siri suar utama, menghasilkan sejumlah 21 suar yang dikaji. Imej dianalisis dan ditafsir dengan menggunakan ImageJ dan Helio Viewer untuk mengukur ciri-ciri suar suria. Penampakan bentuk sigmoidik magnet boleh dilihat dalam imej EIT 195Å manakala MFR boleh dilihat dalam imej magnetogram. Kriteria ramalan kami menyatakan bahawa suar utama terjadi di AR yang mempunyai kelas Zurich D, E atau F, kelas Penumbra K, Kelas kepadatan I dan C, dan kelas Mt Wilson BGD. Ramalan magnetik menunjukkan AR yang tidak akan menghasilkan suar suria utama dengan 99.5% ketepatan dan 98% kepekaan. Kaedah ramalan ini boleh memberi amaran awal bagi

kejadian suar suria utama dalam masa 1-4 hari. Berserta dengan imej MFR dan rajah bentuk sigmoidal, ketepatan ramalan adalah meningkat.



# MULTISPECTRAL STUDY OF MAJOR SOLAR FLARES TOWARD FLARES PREDICTIONS

## ABSTRACT

Major solar flares (X-class) are the most dangerous solar activities for the Earth in terms of space weather. It is due to a magnetic eruption and sudden release of intense magnetic energy at active regions (AR). The main objective of this research is to identify AR characteristics (McIntosh and Mt Wilson class) associated with major solar flares from NGDC data and to formulate criteria for its early prediction. These criteria are enhanced by qualitative multispectral images. Multispectral images such as a continuum, magnetogram, and EIT 195Å images from SOHO were used in this research. This study took into account the evolution of AR, properties of AR (Zurich, Penumbra, Compactness and Mt Wilson class), the morphology of magnetic flux rope (MFR), and formation of magnetic sigmoidal shape. Considering data availability and consistency, we chose five AR, namely AR 10486, AR 9393, AR 9415, AR 10720 and AR 9077 were chosen. Each AR generated series of major flares, resulting in a total of 21 flares studied. Images were analysed and interpreted by using ImageJ and Helio Viewer to measure solar flares features. The appearance of magnetic sigmoidal shape can be seen in EIT 195Å images while MFR can be seen in magnetogram images. The prediction criteria state that major flares occur at AR that has Zurich D, E or F, Penumbra class K, Compactness class I and C, and Mt Wilson class BGD. A negative prediction showed AR that will not produce major solar flares with 99.5% accuracy and 98% sensitivity. This prediction method can give early warning for major solar

flares occurrences within 1-4 days. By including MFR and sigmoidal shape images, the accuracy of the prediction was improved.

## CHAPTER 1

### INTRODUCTION

#### 1.1 The Sun

The Sun is the sole source of energy in term of heat and light for the daily use of the Earth. The Sun is located at the centre of the solar system with 149 million km from the Earth (Raulin and Pacini, 2005). It is a G-type main-sequence star (G2V) based on its spectral class and the dwarf stars. It belongs to the main sequence of the stars (Moussas et al., 2005). The Sun held together by its own gravity and powered by nuclear thermal fusion at its centre. The Sun started its life almost 4.6 billion years ago. Its mass is  $1.9891 \times 10^{30}$  kg and the average radius is 695,700 km. It also considers as blackbody source with temperature 5,700K. The power emitted by every square meter is  $6,329 \times 10^6$  J/m<sup>2</sup>s or 63 GW/m<sup>2</sup>. The Sun have similar physicals and chemicals properties with other stars (Moussas et al., 2005). Thus, stars scattered around the universe can be understood by referring to the Sun properties (Chaisson and McMillan, 2005; Moldwin, 2008)

#### 1.1.2 Structure of the Sun

Generally, the Sun can be divided into two main part which is interior and atmosphere. The interior part is divided into three main zones; core, radiation, and convection zones. The atmosphere part also is divided into three zones; photosphere, chromosphere and the corona.

In interior of the Sun, the thermal nuclear reaction takes place in the core zone that generates and releases a massive ton of energy in every second. The radius of central core roughly 200,000 km. Above core zone is the radiation zone about 300,000 km where the energy is transported through electromagnetic (EM) photon or radiation. Beyond radiation zone which is below photosphere extending down 200,000 km, is the convection zone. The convection zone begins where flux radiation of energy is so high and energy does not efficiently transport through the gas, hence convection zone begins in order to transport the energy through bulk fluid motion like a pot of boiling water. This region undergoes convective motion to transfer heat to photosphere where it can radiate out into space (Moldwin, 2008).

At atmosphere of the Sun, the photosphere is the first layer just above the convection zone. It also called as “surface” of the Sun that emits the radiation to space. Photosphere is very thin probably no more than 500 km. Observation of the Sun shows photosphere is contained spots called “sunspots”. The sunspots are known as the region of the strong magnetic field. They are slightly cooler typically 4,500K compare to the 5,700K of surrounding photosphere due to strong magnetic fields. Sunspots appear darker than surrounding solar surface. Above photosphere is chromosphere. It’s about thickness 1,500 km. The chromospheric temperature is inversely proportional to plasma density and the density of the plasma drops rapidly with the height in the chromosphere. Thus, the outer chromosphere has a high in temperature (Chaisson and McMillan, 2005). Above the chromosphere, there is the transition region in which the temperature is rising dramatically. The outer atmosphere of the Sun is the corona. The corona temperature is very high more than million Kelvin if compared to photosphere and chromosphere. Beyond the corona is the solar wind. The

solar wind is the gas that escapes into interplanetary space. Figure 1.1 shows structure of the Sun.

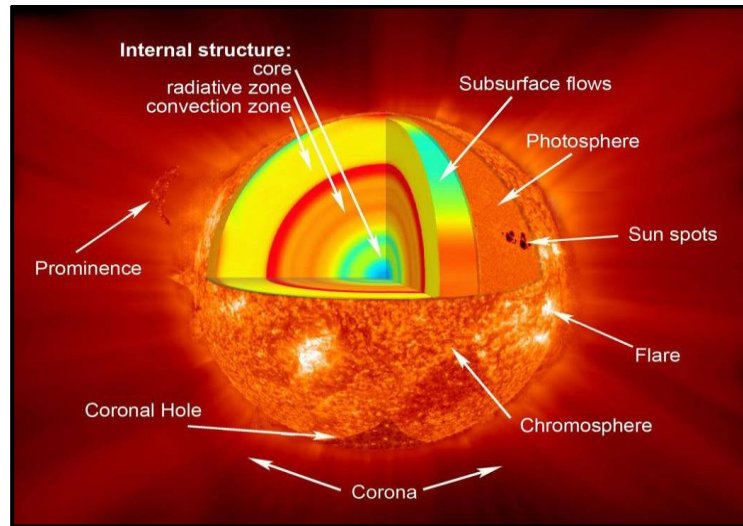


Figure 1.1: Structure of the Sun (Nasa, 2017).

Like the Earth, the Sun also have its own activities called solar activities. Phenomena like active region (AR), sunspots, solar flares, coronal mass ejections (CMEs), high-speed solar wind, and solar energetic particles (SEP) are examples of solar activities. The AR is the region that has strong magnetic field and sunspots usually located at the AR (Gopalswamy, 2003). Most of the solar activities such as solar flares and CMEs are coming from the AR. Both phenomena are affecting the terrestrial environment and could affect our daily life (Colak and Qahwaji, 2009). Solar activities are release solar charged particles at high speed and bombard the Earth magnetic field. Major solar flares associated with CMEs give tremendous effect on the earth that contains  $10^{12}$  kg of material and can move away from the Sun over  $1,000 \text{ km s}^{-1}$  (Youssef, 2012). At this rate, it can lead to space storm, geomagnetic disturbance, disturb GPS signal, increases the drag on Low Earth Orbiting (LEO)

satellites, damage and crippling Earth-orbiting satellite, reducing their lifetime in orbit, disturbance or damages on radio communication and disrupting or blowing up power system on Earth (Koskinen et al., 2001; Zainal et al., 2015). Space weather or space science is a science to study and monitoring all solar activities especially solar flares and CMEs. It also can help the agencies like satellite operators, space agencies, aviation industry, power generation agencies, distribution industry, oil and gas industry, railways and etc to make precaution steps when major solar activity strike the Earth (Moldwin, 2008; Colak and Qahwaji, 2009; Jacobs and Poedts, 2011).

## **1.2 Space weather**

Space weather is emerging field within the space sciences that studies solar activities and the influences of the Sun towards Earth environment and technologies (Moldwin, 2008; Moussas et al., 2005). Space weather is defined by the U.S. National Space Weather Program (NSWP) as conditions on the Sun and in the solar wind, magnetosphere, ionosphere, and thermosphere that can influence the performance and reliability of space-borne and ground-based technological systems and can endanger human life or health (Colak and Qahwaji, 2009; Koskinen et al., 2001).

Similar, space weather is more focus in space. Space begins at the Earth atmosphere called thermosphere, which roughly at 100 km (Moldwin, 2008). The concern about space weather is increasing for two reasons. First solar activities affect life on Earth and second too much depend on communications and power systems. Both are too sensitive to space weather (Qahwaji and Colak, 2007; Colak and Qahwaji, 2009). The best method for prediction solar activities, especially solar flares is to give the real-time early warning and the possible effects to the Earth. In this way, the initial

precaution step can be done by the agencies concerned (Colak and Qahwaji, 2009; Wang et al., 2004; Papathanasopoulos et al., 2016)

Multispectral study of solar flares and CMEs are important in space weather forecasting and help deep understanding the solar flares and CMEs process (Gopalswamy and Thompson, 2000; Choudhary et al., 2013). The current prediction system for solar flares and CMEs are depend on the Large Angle and Spectrometric Coronagraph Experiment (LASCO) observations and Geostationary Operational Environment Satellites (GOES). If both satellites are breakdown, then solar flares and CMEs monitoring becomes impossible. For that reason, it is necessary to study and analyse the solar flares and CMEs in different observational or another suitable techniques (Zhu et al., 2016 and Wang et al., 2006).

### **1.3 Problems statement**

Major solar flares (X-class) are the most dangerous solar activities in terms of space weather and has a direct impact on the Earth in term of technology and our daily life. It is due to a magnetic eruption and sudden release of intense magnetic energy at active regions (AR). Major solar flares can release changes particles that contain  $10^{12}$  kg (electrons and occasionally protons) with high speed around  $1,000 \text{ km s}^{-1}$ . With this condition it will cause geomagnetic storm and space storm to the Earth. Thus, monitoring and prediction of solar flare are important to protect our technology especially satellite communications since we in the modern world rely too much on satellite communications nowadays. Researcher around the world attempted to build a prediction and monitoring systems to predict solar activities especially solar flares. However, the system is good to predict lower/minor class solar flares (A, B, C, and

M) but it becomes less accurate and unpredictable for major class solar flares (X-class).

Therefore, this research aims to build a prediction method for major solar flares only by using observation data of AR characteristics (McIntosh and Mt Wilson classification systems) and assisted with multispectral images data (continuum, magnetogram, and extreme ultra violet spectrum). This research focuses on major solar flares because it has 90% associated with CMEs.

#### **1.4 Research objectives**

1. To identify the active region (AR) and study their characteristics with respect to major solar flares from archive data.
2. To analyse images from several wavelength ranges (continuum, magnetogram, and EUV) of identified major solar flares before, during and after major flares.
3. To give early criteria of major solar flares for prediction method and monitoring purposes.

#### **1.6 Research scope**

Firstly, this research focus on identifying AR properties that producing major flares by using numerical data from National Geophysical Data Center (NGDC). 21 major solar flares within five AR were selected in this research. The characteristics of the AR such as the evolution area, Zurich, Penumbra, Compactness ( $Z_{pc}$ ) class are considers in this research study. With all these data, the trend of the major flares can be seen by plotting the graph against date. Secondly, this research focus on solar flares features in multispectral images by using continuum, magnetogram, and extreme



ultraviolet images telescope (EIT 195Å) from Solar and Heliospheric Observatory (SOHO). AR morphology can be seen clearly through continuum images, magnetic flux rope (MFR) can be seen through magnetogram images and the solar flares eruption, sigmoidal shape, and arcade formation can be seen through EIT 195Å images. By combining numerical and images data, correlation of solar flares can be seen clearly. Lastly, this research focuses on prediction method based on selected criteria from numerical data and assisted by images data.

## **1.7 Thesis layout**

The overall structure of the study contains 5 chapters, including introduction, literature review, data collection and methodology, result discussion, conclusion and some recommendation for future research studies. The research layout are as follows:

**Chapter 1** begins with a brief introduction of solar flares impact on the Sun and space weather. This chapter also contains the problem statement and the objective of the research study.

**Chapter 2** is the literature review of the solar activities related to the solar flares. This chapter also discusses details on active region characteristics, solar flares features in multispectral observation and current technology for predicting solar flares.

**Chapter 3** is more focusing on the methodology of the research starting from the data collection, processing, selected criteria of major solar flares and prediction method. There are two types of data that have been used which are numerical data and images data. This chapter also explained the important steps during data analysis for both types of data.

**Chapter 4** will be explained the result from the methodology. The discussion is more discussing the numerical and images data that containing the characteristic of each active regions (AR) towards solar flares occurrences. This chapter also explain on how the early criteria of solar flares ware selected and used in prediction method. The evaluation of prediction method is also be discussed in the chapter.

**Chapter 5** is the summary of key results and discussion in previous chapter and concludes all the research objective. Recommendation for future research based on current technology to gain the understanding of solar flares are also suggested in this chapter.

## CHAPTER 2

### LITERATURE REVIEW

#### 2.1 Solar activities

Solar activities are any activities that occur at the Sun especially at Sun atmosphere. Solar activities represent active regions (AR), sunspots, flares, coronal mass ejections (CMEs) and other solar eruptive events. These activities will produce massive amounts of radiation, high energy particles (electrons and sometimes protons) and high-speed solar plasma (as solar wind) to the interplanetary space. It has been revealed that solar atmosphere has more aggressive and dynamics especially in solar corona (Kivelson and Russell, 1995; Foukal, 2008). One of the primary findings is magnetic reconnection occurs all around the Sun to caused dynamic phenomena like nanoflares, picoflares, microflares, coronal jets, shock waves at solar atmosphere, etc (Magara and Shibata 2008). Many data from high-resolution observations show solar flares and CMEs are due to magnetic reconnections that lead to solar eruption (Veselovsky and Panasenco, 2006). The magnetic reconnections are the main causes of solar activities. Now it is accepted that magnetic reconnection causes various kinds of solar activities especially solar flares and CMEs. These phenomena can affect the Earth's upper atmosphere (Papathanasopoulos et al., 2016).

Earth is sheltered from the solar activities by its magnetosphere. However, under a certain situation like solar flares and CMEs, it can pass through the terrestrial environment and disturb the Earth magnetosphere. This will lead to geomagnetic activity (magnetic storms) on the Earth (Belov et al., 2014; Papathanasopoulos et al., 2016). Many solar activities forecasting techniques and systems have been developed

based AR morphology, solar flares, and CMEs characteristics to understand the patterns of the activities (Kivelson and Russell, 1995; Yuan et al., 2010). Active region, solar flares and CMEs phenomena have a deep interest in solar and geophysical scientists since both phenomena give direct impact to everyday life on Earth (Delaboudini et al., 1998; Sterling et al., 2000).

### **2.1.1 Active Region (AR) and Sunspots**

The active region (AR) and sunspots are the main aspects of producing solar activities. Sunspots are emergence as dark spots on the solar photospheres. An active region is a region on the photosphere that has a strong magnetic field and most of the solar activities come from the AR due to the strong magnetic field (Sterling et al., 2000; Nguyen et al., 2006). Sunspots usually form in AR. AR characteristics are widely used for forecasting solar activities (Colak and Qahwaji, 2007a). AR is originated from magnetic activity in the interior part of the Sun and emergence at photospheres. The AR start with a combination of magnetic field lines from small pores. When two of these pores combine with one another, they compress the plasma between them into a long structure called a light bridge. Finally, the light bridges combine with each other (light bridge) to become a single large sunspot or active regions (Hathaway and Choudhary, 2008).

A single sunspot usually forms in one or more dark cores, called umbrae and generally surrounded by a less dark area called penumbra. Umbrae have very strong and longitudinally align of magnetic fields that make the sunspots regions to become relatively cool. The Figure 2.1 shows the example of single sunspots with umbra and penumbra.

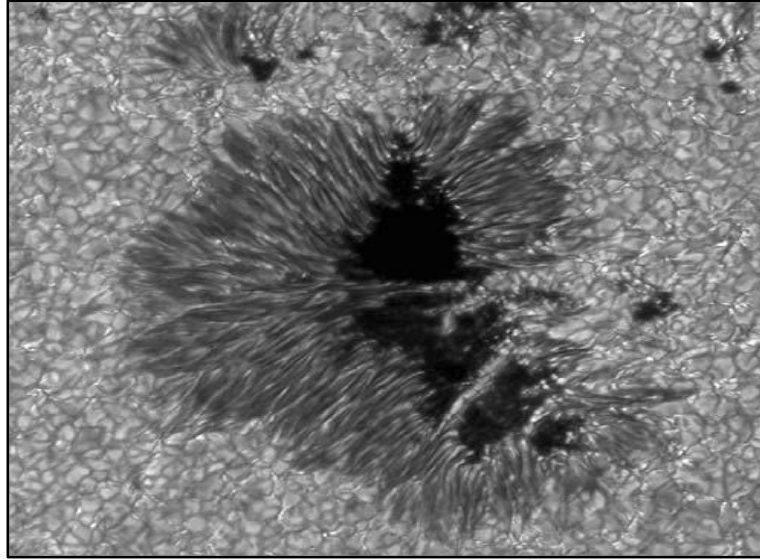


Figure 2.1: The central dark part of the sunspots is the umbra. The radially striated part is the penumbra. The surrounding bright cells are granular convection cells (Solanki, 2003).

AR also experience a proper motion due to the differential solar rotation, growth and expansion of the magnetic flux. When an AR reached its maximum longitudinal extent, it generally stable or starts to decay as the magnetic field is weakening (McIntosh, 1990; Nguyen et al., 2006). AR is also having a life-cycle. They are form groups and formations, born and die, grow and decay in size, and rotated across the Sun's surface around their lifetime (Nguyen et al., 2006). With the advanced telescopes and photographic devices, a theory about AR and their relation to other solar activities phenomena has increased. Analysis and classification of sunspots in the AR are a crucial part of gaining the knowledge about space weather (McIntosh, 1990; Sterling et al., 2000; Nguyen et al., 2006).

For this reason, AR and sunspot are systematically classified into two main class which are McIntosh classification systems and Mount Wilson classification system that allows observatories around the world to report the data uniformly. Previous research on solar flare shows that they are frequently associated with the AR

and sunspots characteristics (Smith and Howard, 1967; Qahwaji and Colak, 2007; Wang et al., 2008). In order to investigate this relationship, McIntosh classification systems (Zpc) and magnetic configuration through Mount Wilson classification system are used to study the correlation towards solar flares (Smith and Howard, 1967; McIntosh, 1990). Both classification systems will be explained future in the next subtopics.

### **2.1.1(a) Zurich Classification System**

Zurich classification system used for classifying the AR to a specific class. Zurich classification system was introduced by Cortie (1901) and develop by Waldmeier in 1947 (McIntosh, 1990). Zurich classification system is widely used in 1966. However, this system has some deficiency in term of structural and dynamical of AR which are related to solar flares events (Smith and Howard, 1967; McIntosh, 1990). Thus, a new McIntosh classification system was introduced to replace old Zurich classification systems. This new McIntosh system is adopted as regular interchanges of solar-geophysical data (Smith and Howard, 1967; McIntosh, 1990).

### **2.1.1(b) McIntosh Classification System**

McIntosh classification system is a new modified system from old Zurich classification system to classify AR into a specific class. This classification system was introduced in 1966 and has been used until now (Qahwaji and Colak, 2007). McIntosh system has 3 main components. First, new modified Zurich (Z) class. The second component is the type of Penumbra (P) class of the biggest spot in AR and third component is a degree of Compactness I class in the interior groups. Thus, the

general form of McIntosh classification is “Zpc” class (Zurich, Penumbra, and Compactness).

The advantage of McIntosh classification is it can reduce a large and complex form of AR into small and simple groups. By that, the study of correlation AR and solar flares can be improved (McIntosh, 1990). Figure 2.2 illustrates the McIntosh class with three main components of Zpc. All this classification only required white light observation and the magnetic classification is not necessary to differentiate the McIntosh class (McIntosh, 1990; Nguyen et al., 2006).

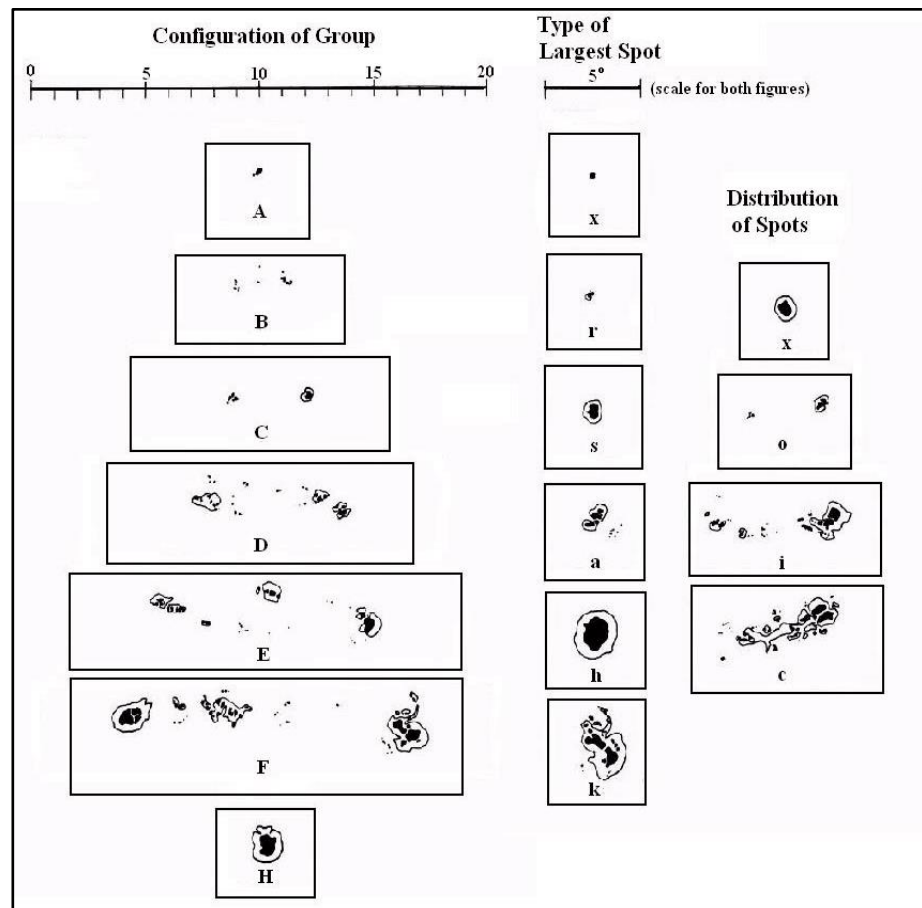


Figure 2.2: The 3 component McIntosh classification with examples of each category. The first column is Zurich class, the second column is Penumbra class and the third column is Compactness class (Nguyen et al., 2006).

### 2.1.1(b)(i) Modified Zurich Class – Z

The old Zurich class was modified in order to improve the correlation of solar flares. The Zurich class is defined as the existence of penumbra and the length or longitudinal extent between the outermost of the AR group leader and follower of the spots (McIntosh, 1990; AFWAMAN, 2003). Figure 2.3 shows the example of longitudinal extent measurement. The complexity of penumbra is not taken into account. The old Zurich classes consist of G and J but both of the classes were removed in the new McIntosh system because they can be described by a combination of new modified Zurich class (McIntosh, 1990). Figure 2.2 shows typical examples of each Zurich class. There are seven classes and each of the classes represents the evolution state of AR groups. Table 2.1 explains the modified Zurich classification (McIntosh, 1990; AFWAMAN, 2003).

Table 2.1: The definition of modified Zurich class (AFWAMAN, 2003).

Modified Zurich Class	Definitions
A	The unipolar group with no penumbra, at start or end of spot group life. The length is (normally) less than 3 heliographic degrees.
B	The bipolar group with no penumbra; length is (normally) 3 heliographic degrees or greater.
C	The bipolar group with penumbra on one end of the group, usually surrounding largest of leader umbrae.
D	The bipolar group with penumbra on spots at both ends of the group, and with longitudinal extent less than or equal to 10 heliographic degrees (120,000 km).
E	The bipolar group with penumbra on spots at both ends of the group, and with longitudinal extent is greater than 10 but less than or equal to 15 heliographic degrees.
F	The bipolar group with penumbra on spots at both ends of the group, and length more than 15 heliographic degrees (above 180,000 km).
H	The unipolar group with penumbra. The principal spot is usually the remnant leader spot remaining from an old bipolar group.



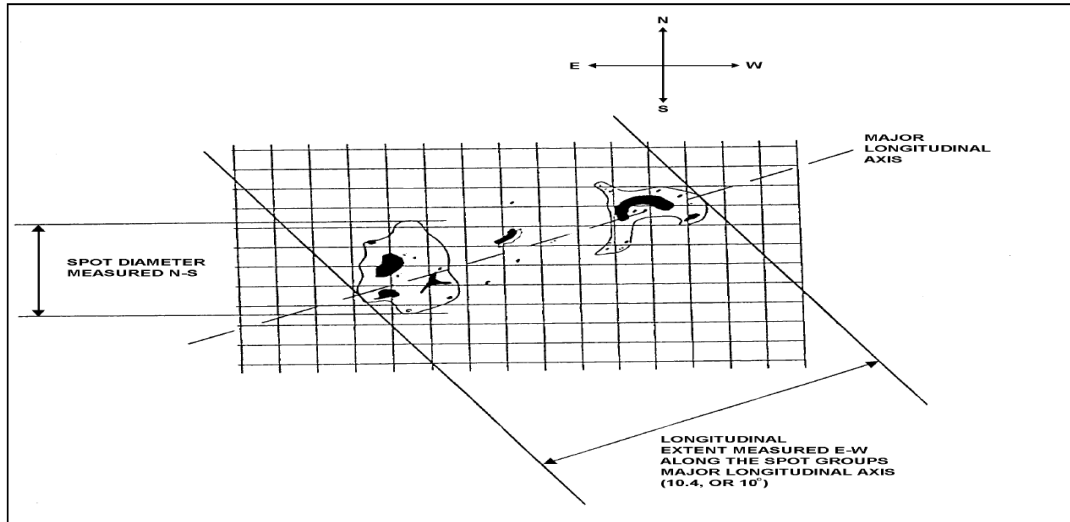


Figure 2.3: Sunspots group length measurement and penumbra diameter (AFWAMAN, 2003).

### 2.1.1(b)(ii) Penumbra Class – P

The second element in McIntosh classification is the Penumbra class. Penumbra class describes the largest spot in AR. Penumbra is the grey area bordering the black umbra. If an apparent grey area is too indistinct to be drawn, it should not be reported. Penumbra class is illustrated in the second column in Figure 2.2. The class description of penumbra consists of size, maturity, stability, and complexity. Table 2.2 explains the definition of Penumbra class (McIntosh, 1990; AFWAMAN, 2003).

Table 2.2: The definition of Penumbra class (AFWAMAN, 2003).

Compactness class	Definitions
x	No penumbra
r	Rudimentary penumbra. Incomplete, irregular penumbra. It is brighter than mature penumbra and has a mottled or granular (vice filamentary) fine structure.
S	Small symmetric penumbra. Mature, dark, circular or elliptical penumbra with filamentary fine structure, and an N-S diameter across the penumbra of 2.5 heliographic degrees or less.
A	Small asymmetric penumbra. Mature, dark, irregular penumbra with filamentary fine structure, and an N-S diameter across the penumbra of 2.5 heliographic degrees or less. The asymmetry is “real”, not just due to foreshortening effects.
H	Large symmetric penumbra. Has the same characteristics as an (s) class penumbra, but with an N-S diameter across the penumbra greater than 2.5 heliographic degrees.
K	Large asymmetric penumbra. Has the same characteristic as an (a) class penumbra, but with an N-S diameter across the penumbra greater than 2.5 heliographic degrees.

### 2.1.1(b)(iii) Compactness Class – C

The third element in McIntosh classification system is the Compactness class of sunspot distributions. Compact class is referring to the density of a spot population in internal active regions. There is five class that limited to bipolar groups according to its sample ranking (McIntosh, 1990; AFWAMAN, 2003). Furthermore, this simple racking helps to identify the of the area group, the condition of a spot either its early birth or mature spot and helps to identify the strong spots near polarity inversion line between leader and follower spots (Warwick, 1965). Figure 2.2 show the examples of

compactness class in the third column. The definition of compactness class is explained Table 2.3.

Table 2.3: The definition of Compactness class (AFWAMAN, 2003).

Compactness class	Definitions
x	Undefined for a single spot or unipolar spot group.
O	Open. Few or any spots between the leader and follower spots. Any interior spots are very small umbral spots or pores.
I	Intermediate. Many spots lie between the leader and follower portions of the group, but none of them possesses mature.
C	Compact. The area between the leader and follower ends of the spot group is located with many strong spots at least one interior spot possessing mature penumbra.

The McIntosh combination of modified Zurich, Penumbra, and Compactness class have limited the number AR formation to 60 combinations. Table 2.4 shows the allowed combination for McIntosh classification (McIntosh, 1990; Nguyen et al., 2006).

Table 2.4: Allowed types group in McIntosh classification system (AFWAMAN, 2003)

Zurich Class	Penumbra Class	Sunspot Distribution	Number of Combinations
A	x	x	1
B	x	o, i	2
C	r, s, a, h, k	o, i	10
D, E, F	r	o, i	6
D, E, F	s, a, h, k	o, I, c	36
H	r, s, a, h, k	x	5
		Total allowed types	60

The evolution pattern of AR almost similar for most sunspot groups. Its begin with single tiny spot umbra or compact spot group joined with another same group usually have opposite magnetic polarity from the first group with separated 3 heliographic digress (approximate  $3 \times 10^4$  km) in a few hours later. The merging a tiny spot (umbra) group together usually will develop into a large leader spots and it will surround by penumbra (McIntosh, 1990).

At the same time, the AR forms few larger spots at the opposite end of the AR (called following). Both group (leader and follower) spots groups are continuing to grow until the penumbra and large spots are emerging at the interior of the AR. The peak area and maturity of AR are commonly shown in less than a week (Nguyen et al., 2006).

The decay process of AR starts when the mature AR is detachment and disjunction of the following spots until remains only a leader spot. Around a week, the remaining spot losses penumbra structure and decay back to a single spot like early life. The birth and death of sunspot in AR are different depends on size and motion of the spots (McIntosh, 1990).

Larger sunspots groups have a similar structure to small isolated groups. The sunspots groups can maintain and continue to grow through the consecutive emergence of multiple bipolar group spot within AR. The expansion and motion of bipolar sunspots lead to merging among bipolar area and resulting very complex geometries of AR (Smith and Howard, 1967; Nguyen et al., 2006).

### 2.1.1(c) Mount Wilson Classification

Mount (Mt) Wilson class is the magnetic class configuration of AR that may get from computer-generated magnetic maps, manual drawing inversion line analysis or any other suitable observation technique can be used (AFWAMAN, 2003). The magnetic polarities and plage distribution within sunspots is the important basis for this classification. In general, there are three main classes which are Alpha (A, unipolar), Beta (B, bipolar), and Gamma (G, complex) (Smith and Howard 1967; McIntosh, 1990; AFWAMAN, 2003). The definition of each class will explain in table 2.5.

Sub-classification Delta (D) class is a special magnetic configuration. The D classification is not clearly described. It exists when one or multiple umbra that have two opposite magnetic polarity separated by polarity inversion line (PIL) within the same penumbra with their boundary separated by no more than 4 heliographic degrees. They usually round, compact and most likely to occurs in large sunspot that has strong magnetic fields (Warwick, 1965). The D class configuration has twisted field line and high field gradients characteristics (Sammis et al., 2000). It is huge and has 80% probability to produces flares (Warwick, 1965). Figure 2.4 shows the example of the magnetic configuration of Mt Wilson class.

Table 2.5: The definition of Mt Wilson class (AFWAMAN, 2003).

Mt Wilson Class	Definition
Alpha (A)	A unipolar sunspot groups.
Beta (B)	A sunspot group having both positive and negative magnetic polarities bipolar with a simple and distinct division between the polarities.
Gamma (G)	A complex AR in which the positive and negative polarities are so irregularly distributed as to prevent classification as a bipolar group. A spot group in which the polarities are completely intermixed.

Table 2.5: Continue

Mt Wilson Class	Definition
Beta-Gamma (BG)	A spot group that has Beta (bipolar) characteristics but is lacking a well-defined dividing line between regions of opposite polarity. This class includes cases in which spots of the opposite or “wrong” polarity accompany the leader or follower regions
Delta (D)	A qualifier to magnetic classes indicating that umbrae separated by less than 4 degrees within one penumbra have opposite polarity
Beta-Delta (BD)	A spot group, which has Beta characteristics, but has umbrae of opposite polarity inside the same penumbra.
Beta-Gamma-Delta (BGD)	A spot group, which has Beta-gamma characteristics, but has umbrae of opposite polarity inside the same penumbra.

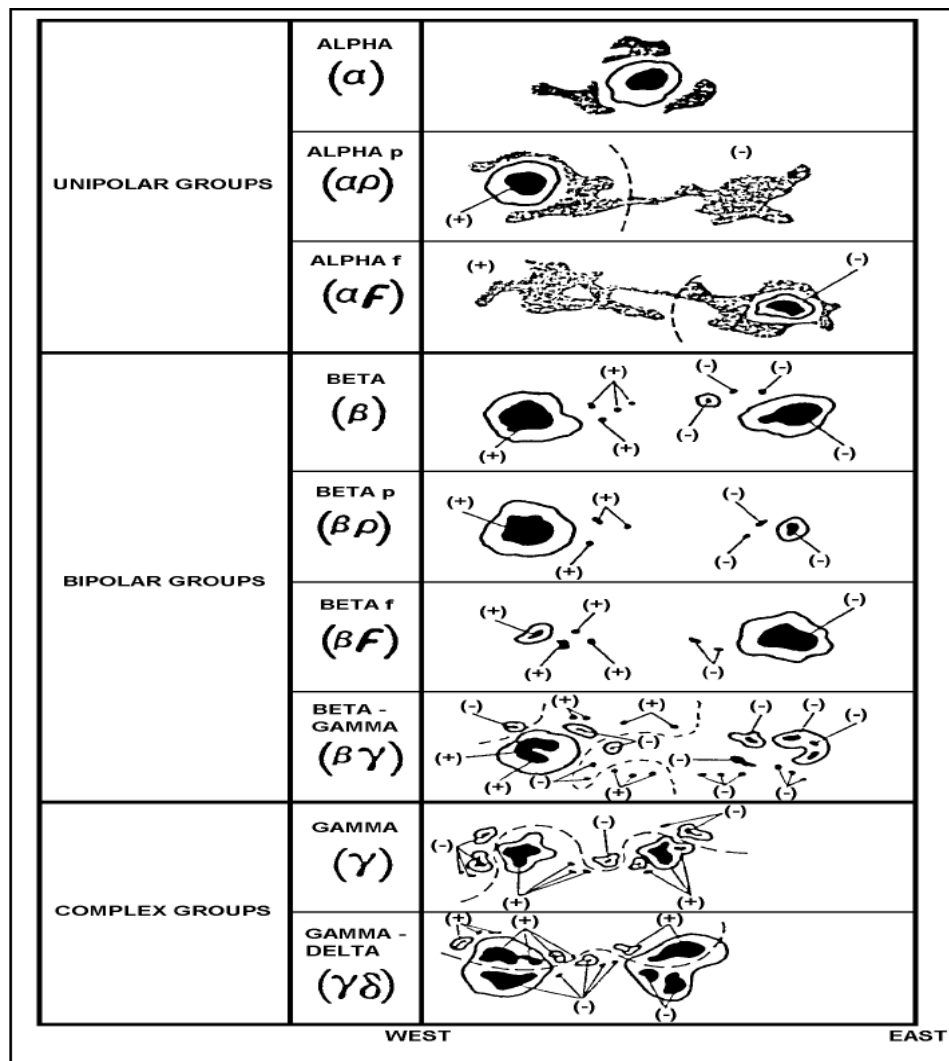


Figure 2.4: Example Mt Magnetic classification system.

### **2.1.2 Relationship between McIntosh and Mt Wilson Class towards major flares**

The relationship between the evolution of AR characteristics and solar flare productivity are crucial element to develop space weather prediction systems (Choudhary et al., 2013). Early observations show solar flares often occur at the same location as magnetic flux emergence at the AR (Dodson and Hedeman, 1970; Sammis, et al. 2000). Statistics data shows solar flares activities have a strong relationship to the complexity of AR characteristics and magnetic configurations especially AR with D type magnetic configuration (Smith and Howard, 1967). The D class configuration is very active and most of the major solar flare coming from D class due to magnetic flux twist or flux emergence among the others spots (Green et al., 2003; Tian and Liu, 2003; Choudhary et al., 2013). The D type likely has a sharp gradient in the current sheet where the flares occur. By observation, the flash during impulsive phase occurs along the magnetic polarity inversion line (PIL) and PIL is located where D class shows it characteristics (Zirin and Tanaka, 1973; Smith and Howard, 1967; Sammis et al., 2000; Deng et al., 2011). The D class is an important parameter for solar flares problems and it becomes an indicator of space weather application (Sammis et al., 2000). Künzel, (1959) original ideas state that AR that has BGD magnetic configuration produce many more strong flares other than the magnetic class of comparable size. Nearly 40% of major solar flares have BGD class configuration properties (Qahwaji and Colak, 2007).

Furthermore, the growth phase of AR has a high flares index compared to the decay phase. This agrees with the early finding that sudden changes in the AR area during growing phase have high potential to produce more solar flares with pre-maximum growth. This is the reason most of the solar flares are produce more flares

per unit area towards mature AR compared to unipolar sunspots which not produce any flares (Sammis et al., 2000; Choudhary et al., 2013). The new of magnetic configuration during growth phase also increase in producing solar flares (Lee et al., 2006; Choudhary et al., 2013). Modern observations using magnetograms images shows the magnetic field configurations are changing rapidly at the AR. This might result from the penumbra field relaxing upward by reconnecting magnetic fields above the surface of the AR (Sudol and Harvey, 2005; Deng et al., 2005, 2011; P. Wang et al., 2011).

Most of flares and CMEs occur during and/or after new flux emergence due to magnetic flux imbalance. The magnetic flux imbalance causes by the photospheric electric current in the field structure that will produce a magnetic field in several directions and long distance connection through field lines (Green et al., 2003; Tian and Liu, 2003). Moreover, the diffused nature behaviours of one spot polarity to another spot will make a magnetic flux imbalance. Thus, the sudden emergence of magnetic flux in pre-existing magnetic field structure and instability of large-scale magnetic fields can lead to large flares and CMEs (Tian and Liu, 2003; Choudhary et al., 2013).

Moreover, the large AR area usually has high potential to produce major solar flares and strong CMEs, but it may not produce any major solar flares and CMEs at all. This is due to low of free energy in the AR. This situation can be applied to small AR that has low potential energy, but it has high free energy, thus small AR could produce major solar flares and strong CMEs. Many solar flares have been observed have free energy that exceeds 50% of total energy (Green et al., 2003; Choudhary et al., 2013; Li and Zhu, 2013). Free energy is the energy stored in the magnetic field at



the AR that has to exceed the potential magnetic field energy. Also, can be defined as the differences in total magnetic energy ( $E_o$ ) and the potential magnetic energy ( $E_p$ ).

Hence, the flare probabilities are higher during growth phase (Sam et al., 2000; Lee et al., 2006; Choudhary et al., 2013), a region that high photospheric magnetic flux imbalance and long polarity inversion lines (PIL) that have highly variable distribution of shear along their length (Leka and Barnes, 2007; Cui et al., 2007), have free energy that exceed of 50% of total energy (Green et al., 2003; Choudhary et al., 2013; Li and Zhu, 2013) and a high fractal dimension of the photospheric field (Ireland et al., 2008; Fletcher et al., 2011).

## **2.2 Solar flares**

Solar flares are a magnetic eruption and sudden release of intense magnetic energy that occur at the AR (photosphere) and lasting from tens of seconds (impulsive) to a ten of minutes or hours (gradual). Also, can define as a sudden, rapid and intense variation in brightness. Solar flares produce a burst of radiation in electromagnetic (EM) wave from radio wave to X-rays and sometimes going to gamma rays (Savcheva et al., 2015). Major Solar flares release changes particles that can be detected when approaching towards the Earth (Chowdhury et al., 2015). Generally, solar flares have three main phases which are an early phase (pre-flare), impulsive phase (Siarkowski et al., 2009; Savcheva et al., 2015) and gradual phase (Hudson, 2011). The arcade formation and long decay event (LDE) flares can be observed in gradual phase. Gradual phase is referred to “post-flare loops” (Siarkowski et al., 2009; Kennedy et al., 2013), “arcade formation” or “post-eruption arcade” (Siarkowski et al., 2009; Joshi et al., 2011).

Solar flares are classified according to X-ray intensity in wavelength range 1 to 8 Angstroms ( $\text{\AA}$ ) measured by Geostationary Operational Environmental Satellites (GOES) according to the power of the X-ray flux peak classification (Bellotti et al. 2013). There are five flares class all together which are A, B, C, M, and X. Every class has 9 subs level except for X class. For example, solar flares class B2.0, C5.8, M7.1, X17 etc. The dangerous flares are solar flares X class (major flares). It can be going up to solar flares X20.0 (Gopalswamy, 2010). Every class has different consequences on Earth (Qahwaji and Colak, 2007). Table 2.6 shows the solar flares class with intensity and its effect towards Earth.

Table 2.6: The solar flares class and its effects toward Earth.

Solar Flares Class	Peak ( $\text{W/m}^2$ ) between 1 and $8 \text{\AA}$	Effects
A	$I < 10^{-7}$	The lowest class of solar flare. No harmful effects on the earth. The background flux is often in the B-range during solar maximum and in the A-range during solar minimum.
B	$10^{-7} \leq I < 10^{-6}$	
C	$10^{-6} \leq I < 10^{-5}$	Known as minor solar flares and sometimes produces the slow CME. Rarely cause a significant geomagnetic disturbance here on Earth.

Table 2.6: Continue

Solar Flares Class	Peak (W/m <sup>2</sup> ) between 1 and 8 Å	Effects
M	$10^{-5} \leq I < 10^{-4}$	Medium-large solar flares may cause radio blackout and radiation storms. Strong, long duration M-class solar flares are likely to produce a CME. There is a high probability resulting geomagnetic storm.
X	$I \geq 10^{-4}$	The strongest solar flare can cause radio blackout, strong geomagnetic storming (G4 or G5) and powerful CMEs.

Major flares (X class) are complex phenomenon occurs in a solar atmosphere with many different mechanisms. Major solar flares have strong influence interplanetary and terrestrial space by shock hard EM radiation, strong energetical particles (SEP), accelerated particles etc (Somov et al., 2003; Yuan et al., 2010; Gopalswamy, 2010).

### 2.2.1 Theories of solar eruptions

With the advanced development of observation techniques and theoretical studies, a lot of theoretical models had been developed in order to explain the observed phenomena on how the process of a solar eruption that leads to solar flares and CMEs. However, to find the definite model for solar flares and CMEs are still difficult (Valori et al., 2016; Kumar et al., 2011). Almost all researcher agree solar eruptions are due to magnetic destabilization at the AR, but the mechanism of the eruption like energy